

## Neutron Capture Cross Section Measurements Using a Lead Slowing-Down Spectrometer

N. Thompson, A. Lewis, E. Blain, A. Daskalakis, and Y. Danon

*Gaerttner Linear Accelerator Center, Rensselaer Polytechnic Institute, 110 8<sup>th</sup> St., Troy, NY 12180, [thompn4@rpi.edu](mailto:thompn4@rpi.edu)*

## INTRODUCTION

Accurate simulations of nuclear interactions require accurate nuclear data. This work aims to further develop the method of using a Lead Slowing-Down Spectrometer coupled with a pulsed neutron source to measure nuclear data [1], in this case, neutron capture cross sections. In order to further develop this method, simulations were run using the Monte Carlo N-Particle Transport (MCNP) suite of codes [2] [3] to design the detectors and experiments, and some of these experiments were performed at Rensselaer Polytechnic Institute (RPI).

## EXPERIMENTAL SETUP

This work uses the RPI Lead Slowing-Down Spectrometer (LSDS) and RPI Linear Accelerator (LINAC) located at the Gaerttner Linear Accelerator Center. The following sections are a brief overview of the various systems and detectors which were used.

## The RPI Lead Slowing-Down Spectrometer

The LSDS (partially shown in Fig. 1) is a 1.8 meter cube of high purity lead with customizable measurement channels and a pulsed neutron source in its center. The RPI LINAC is used to accelerate a pulse of electrons up to 60 MeV, these electrons travel through an evacuated tube until they hit a tantalum target in the center of the lead where neutrons are produced by  $(e,\gamma)$  and  $(\gamma,n)$  reactions in the target. Neutrons produced have an energy distribution that can be approximated as Equation 1, an evaporation spectrum with a peak energy of 0.46 MeV [4]:

$$\phi(E) = C * E * e^{\left(\frac{-E}{b}\right)} \quad (1)$$

where  $C$  is a normalization constant,  $E$  is the neutron energy in MeV and  $b$  is 0.46 MeV.

Since electrons are produced with a 250 ns pulse width, the neutrons are produced in a similarly short period of time. As neutrons leave the target, they begin to lose energy by scattering with the lead. Due to the large atomic mass of lead in comparison to a neutron, the average lethargy gain (energy loss) in a collision is quite small, meaning it takes a large number (hundreds) of scattering interactions for the neutrons to slow down to thermal energies. This leads to a correlation between slowing down time (the amount of time after the

production of neutrons) and average neutron energy, which can be modeled as Equation 2 [4]:

$$E = \frac{k}{(t-t_0)^2} \quad (2)$$

where  $k \approx 165000 \text{ eV} \cdot \mu\text{s}^2$ ,  $t_0 \approx 0.3 \mu\text{s}$ ,  $t$  is the slowing down time [ $\mu\text{s}$ ], and  $E$  is the average neutron energy [eV]. This time-energy correlation is similar to a Time of Flight experiment with a 5.6 m flight path [5]. As the neutrons are slowing down, the energy distribution of the neutrons can be approximated by Equation 3, an energy dependent Gaussian distribution [6]:

$$\left[\frac{dE}{E}\right]_{FWHM} = \left[0.0835 + \left(\frac{0.128}{E}\right) + 3.05 \cdot 10^{-5} E\right]^{1/2} \quad (3)$$

where  $[dE/E]_{FWHM}$  is the full width half maximum energy resolution, and  $E$  is the neutron energy in eV. The energy resolution is 30% between 10 eV and 1 keV.

Detectors can be placed in channels in the LSDS, such that when a neutron is captured by the sample, the detector will detect some of the cascade of gamma rays that are emitted as a result of the capture. By recording when these detector signals are collected, capture reaction rate spectrum can be created as a function of slowing down time, which can then be converted to be a function of energy using Equation 2. While using the LSDS, the LINAC is pulsed with a frequency up to 180 Hz, and data from each pulse is normalized to accelerator conditions and summed. During the slowing down process, many neutrons will escape the LSDS and be thermalized in the room. A cadmium cover surrounds the LSDS to prevent these thermalized neutrons from reentering the LSDS.

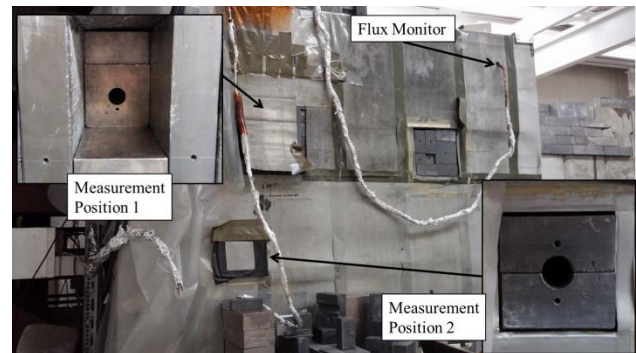


Fig. 1: Photo of the south side of the LSDS with pictures of measurement channels.

### Detector Selection and Setup

In order to perform these measurements, a number of different detector types and scintillator crystals were simulated to assess their performance. These simulations were run with MCNP5 [2] and MCNP6 [3] on the RPI Nuclear Engineering Computer Cluster. Based on these simulations, several detectors were designed and tested using a variety of scintillator crystals. The scintillator crystals tested were PWO (lead tungstenate), YAP (Yttrium aluminum perovskite doped with cerium), and LYSO (Lutetium-yttrium oxyorthosilicate doped with cerium) all with a 0.75 inch diameter and a 15 mm thickness. These were mounted to three different types of Photomultiplier Tubes (PMTs), a Hamamatsu R762, a Photonis XP1911, and an Electron Tubes 9111WB. Also tested was an Eljen EJ-315  $C_6D_6$  (Deuterated Benzene) liquid scintillator where the scintillator had dimensions of 2 inches diameter by 2 inches thick.

The LSDS has a number of channels where bricks of lead can be removed and replaced with bricks of other shapes. Three channels were modified, one to fit the  $C_6D_6$  detector (2 inch by 2 inch by 16 inch channel), and two channels to fit the smaller detectors (1 inch diameter hole, 16 inches deep). Detectors were placed in these channels, with the sample to be measured affixed to the end of the detector. For collecting data, a nanosecond resolution Time-of-Flight (TOF) clock was used. In order to take into account varying beam conditions, a  $^{235}U$  probe fission chamber was also placed in the LSDS, away from the experiments, to act as a neutron flux monitor.

### RESULTS

Measurements were made of tantalum and molybdenum samples. The LINAC was run at 90 Hz with a pulse width of 253 ns and an electron energy ranging from 53.5 to 55 MeV. The YAP scintillator had the best signal to background ratio, and performed the best overall. However, at short slowing down times (under 40  $\mu s$  / above 100 eV), the scintillator was overwhelmed with pulses, leading to a very high detector deadtime. Fig. 2 is a plot of the YAP detector response for the simulation and experiment as a function of slowing down time for a 40 mil (0.10 cm) thick, 1.7 gram sample of  $^{181}Ta$ .

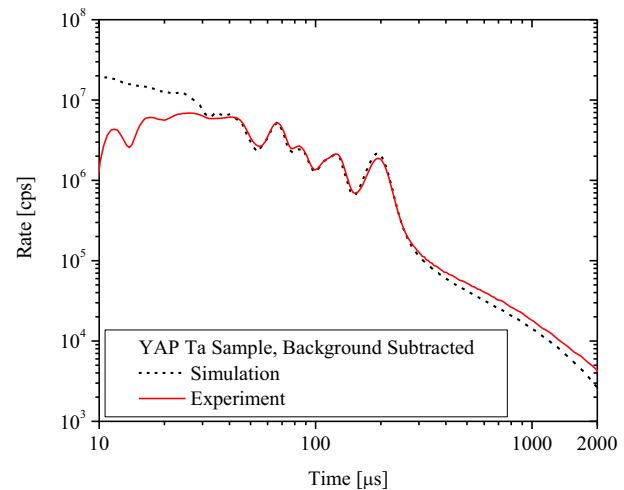


Fig. 2. YAP detector response with a tantalum sample, background subtracted as a function of slowing down time.

By using Equation 2, Fig. 2 can be translated from a function of time to a function of energy. Fig. 3 is a plot of the same data as a function of energy. As shown in Fig. 4, a plot of the radiative capture cross section of  $^{181}Ta$ , the location of resonances (4.28 eV, 10.34 eV, 23.9 eV, 39.13 eV, 98.32 eV) match well to the energies where peaks are observed in the experiment and simulation. While the location of resonances is correct, due to the energy resolution of the LSDS, the peaks are greatly broadened. A discrepancy between the measurement and simulation was observed below 2 eV and needs further investigation.

The  $C_6D_6$  detector also had a high dead time at short slowing down times, but was able to collect good data slightly before the YAP detector (30  $\mu s$ /180 eV).

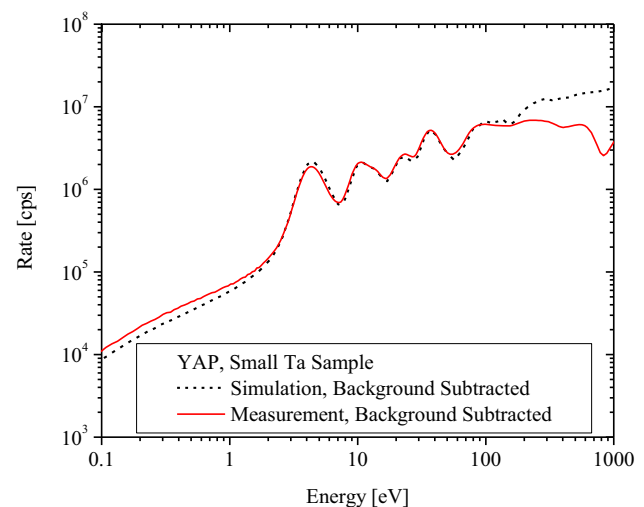


Fig. 3. YAP detector response with a tantalum sample, background subtracted as a function of average neutron energy. ENDF/B.VII.1 (73181.80c) cross section library for  $^{181}Ta$  used in MCNP5 simulation [7].

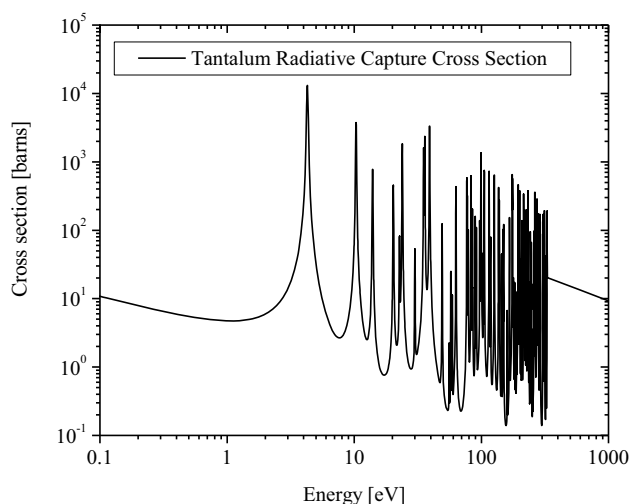


Fig. 4. Radiative capture (MT:102) cross section of  $^{181}\text{Ta}$  (ENDF/B-VII.1) [8].

In both the YAP and  $\text{C}_6\text{D}_6$  detectors, the simulation underpredicted the count rate expected at low energies. One possible source of this difference may be additional moderation of neutrons near the detectors. Electrical tape was used to cover the YAP detector, this additional hydrogen may be leading to more thermalization near the detector. In order to eliminate the use of electrical tape and reduce the amount of hydrogen near the detector, an aluminum cover is being designed to fit over the detector. Another possible source of this discrepancy is room return, or neutrons which have escaped the LSDS being thermalized in surrounding materials and then re-entering the LSDS. A cadmium cover surrounds the LSDS to absorb these neutrons, but it may be useful to surround the measurement channels with additional cadmium to reduce this effect further.

### CURRENT AND FUTURE WORK

The next round of experiments is currently being designed that will take this work a step further. Due to the large count rate at short slowing down times, it was concluded that the scintillators were too large and were collecting too many pulses. A new set of YAP scintillators was purchased that have the same diameter but are thinner (5 mm and 2 mm thick). This should reduce the count rate of the detector substantially and allow for collection of data into the keV region.

Since there is a cascade of multiple gammas emitted from every capture, by measuring with two detectors in the LSDS facing each other with the sample sandwiched between them, coincidence data can be collected. This should greatly reduce the amount of background counts as two background gammas are unlikely to be seen at the same time, which should improve the signal to background ratio. This data is planned to be collected in two ways, with an analog system and a digital system.

### ACKNOWLEDGMENTS

The authors would like to thank the hard work of the LINAC staff (Peter Brand, Matt Gray, Martin Strock, and Azzedine Kerdoun) for keeping the LINAC operating and maintained. The authors would also like to thank the rest of the students, staff, and faculty for their help and expertise. The authors also thank the Stewardship Science Academic Programs for funding this research.

### REFERENCES

- [1] L. PERROT et al, "Precise Validation of Database (n,y) Cross Sections Using a Lead-Slowing-Down-Spectrometer and Simulation from 0.1 eV to 30 keV: Methodology and Data for a Few Elements," *Nuclear Science and Engineering*, vol. 144, pp. 1-15, 2003.
- [2] X.-5. Monte Carlo Team, "MCNP-A General Monte Carlo N-Particle Transport Code, Version 5," *LA-UR-03-1987, Los Alamos National Laboratory*, 2003.
- [3] J. GOORELY et al., "Initial MCNP6 Release Overview - MCNP6 version 1.0," *LA-UR 13-22934, Los Alamos National Laboratory*, 2013.
- [4] N. ABDURRAHMAN, "System Performance and Monte Carlo Analysis of Light Water Reactor Spent Fuel Assay Using Neutron Slowing Down Time Method," *Ph.D. Thesis, Rensselaer Polytechnic Institute*, 1991.
- [5] J. THOMPSON, "A Method for (n,alpha) and (n,p) Cross Section Measurements Using a Lead Slowing-Down Spectrometer," *Ph.D. Thesis, Rensselaer Polytechnic Institute*, 2012.
- [6] B. BECKER et al., "Nondestructive Assay Measurements Using the RPI Lead Slowing-Down Spectrometer," *Nuclear Science and Engineering*, vol. 175, pp. 124-134, 2013;dx.doi.org/10.13182/NSE12-66
- [7] J. CONLIN et al., "Listing of Available ACE Data Tables," *LA-UR-13-21822, Los Alamos National Laboratory*, 2013.
- [8] M. CHADWICK et al., "ENDF/B-VII.1 Nuclear Data for Science and Technology: Cross Sections, Covariances, Fission Product Yields and Decay Data," *Nuclear Data Sheets*, vol. 112, no. 12, pp. 2887-2996, 2011.